A variant histone H3 is enriched at telomeres in *Trypanosoma brucei*

Joanna E. Lowell and George A. M. Cross*

Laboratory of Molecular Parasitology, The Rockefeller University, 1230 York Avenue, New York, NY 10021, USA

*Author for correspondence (e-mail: george.cross@rockefeller.edu)

Accepted 31 August 2004
Journal of Cell Science 117, 5937-5947 Published by The Company of Biologists 2004
doi:10.1242/jcs.01515

Summary

Variant histones play critical roles in transcriptional activation and repression, DNA repair and chromosome segregation. We have identified *HTV*, a single-copy gene in *Trypanosoma brucei* encoding a variant form of histone H3 (H3V). H3V is present at discrete nuclear foci that shift over the course of the cell cycle and associate with the mitotic spindle, a pattern of localization reminiscent of that described previously for both mini-chromosomes and telomeres. By combining fluorescence in situ hybridization with indirect immunofluorescence, we confirmed that the H3V foci overlap with a 177-bp repetitive sequence element found predominantly in mini-chromosomes, as well as with the TTAGGG repeats that compose telomeres. Chromatin immunoprecipitation studies, however, reveal that only the telomeric repeat DNA is substantially enriched with H3V. *HTV* is not essential for viability, mini-chromosome segregation, telomere maintenance or transcriptional silencing at the telomere-proximal expression sites from which bloodstream-form *T. brucei* controls antigenic variation. We propose that H3V represents a novel class of histone H3 variant, a finding that has evolutionary implications.

Supplementary material available online at
http://jcs.biologists.org/cgi/content/full/117/24/5937/DC1

Key words: Histone H3 variant, CenH3, Telomere, *Trypanosoma brucei*

Introduction

The structure and function of a nucleosome can be dramatically altered by a variety of covalent modifications of the individual histones (H2A, H2B, H3 and H4) contained within it (reviewed by Fischle et al., 2003a). Specific modifications, often via interactions with chromatin binding proteins, affect vital processes including transcriptional activation and gene silencing. Such observations have led to the 'histone code' hypothesis, in which combinatorial modifications of histones are thought to extend the information content of chromatin and allow epigenetic information to be retained from one generation to the next (Strahl and Allis, 2000; Fischle et al., 2003b).

Also of critical importance to nucleosome structure and function are variant histones, which substitute for major histones within a nucleosome. Variants corresponding to all four major histones have been identified, ranging from those that contain large non-histone moieties to those that differ from their major histone counterpart at only a few residues (reviewed by Malik and Henikoff, 2003). Although typically representing only a fraction of the total histones, variants play key roles in transcription and in the formation of specialized structural domains of chromosomes. For example, H3.3 and Cenp-A are both variants of histone H3, but have very different properties. H3.3 differs from major H3 at only four amino acids, yet is deposited exclusively at transcriptionally active loci in a replication-independent manner (Ahmad and Henikoff, 2002a). Although its function is not well understood, the importance of H3.3 is emphasized by the observation that it is widely conserved and essential for viability (Ahmad and Henikoff, 2002a; Ahmad and Henikoff, 2002b). Cenp-A, in contrast, is a rapidly evolving histone, sharing only ~50-60% sequence identity with the C-terminal histone fold domain of H3. Cenp-A binds to centromeric DNA and is required for chromosome segregation (reviewed by Henikoff et al., 2001). Cenp-A homologs (CenH3s) have been identified in eukaryotes ranging from those with small, defined point centromeres (*Saccharomyces cerevisiae*) to those with holocentric chromosomes (*Caenorhabditis elegans*), indicating that its function is highly conserved despite extreme differences in centromere organization (Henikoff et al., 2001).

Trypanosoma brucei, the causative agent of African sleeping sickness in humans and nagana in livestock, is a member of the Kinetoplastida, a family of protozoa that diverged early in the eukaryotic lineage (Stevens et al., 2001). *T. brucei* is well known for its sophisticated system of antigenic variation (reviewed by Cross, 1996). In its bloodstream form, the parasite is covered with a coat of variant surface glycoprotein (VSG) and, by periodically switching from one coat to another, avoids elimination by the immune system of the host. Although there are hundreds of distinct *VSGs* scattered around the genome, *VSG* expression is mono-allelic and occurs exclusively at a telomere-proximal expression site. There are ~20 expression sites, but only one is active, and thus a single *VSG* is transcribed. Switching from one VSG coat to another is achieved either by recombination between *VSGs* or via an in situ switch, in which activation of a new expression site is coupled to inactivation of the old expression site (reviewed by

Borst and Ulbert, 2001). Interestingly, the active expression site is present within an expression site body, a non-nucleolar, RNA polymerase I-containing structure that is resistant to nuclease treatment (Navarro and Gull, 2001). When the parasite is ingested by its vector, the tsetse, it differentiates into a procyclic form where all expression sites are shut off and the VSG coat is replaced with one or more members of the small family of 'procyclins' (Roditi et al., 1998).

Remarkably little is known about chromatin and its possible role in VSG expression. The four major histones have been biochemically purified (Bender et al., 1992) and their corresponding ORFs deduced (Horn, 2001). In primary structure, *T. brucei* major histones are highly divergent from model organisms, sharing sequence identity of only ~45-60% with histones from *S. cerevisiae*, for example. Little is known about how *T. brucei* histones are post-transcriptionally modified nor how the 'histone code' hypothesis applies and whether it might be implicated in expression site transcriptional control (Garcia-Salcedo et al., 2003).

The *T. brucei* genome is distributed among several classes of chromosomes that can be distinguished on the basis of size, ploidy and gene composition (reviewed by Ersfeld et al., 1999). There are 11 pairs of megabase chromosomes (MBCs, 1-6 Mbp), several intermediate chromosomes (100-900 kbp) and ~100 mini-chromosomes (MCs, ~50-150 kbp) of uncertain ploidy. Expression sites and arrays of *VSGs* are present at both MBCs and intermediate chromosomes, whereas housekeeping genes reside only within MBCs. In contrast, MCs often contain a single, promoterless *VSG* and are otherwise mainly composed of a 177-bp repetitive sequence (Weiden et al., 1991). All classes of chromosomes are capped with telomeres that form T-loops in vivo (Munoz-Jordan et al., 2001).

The mitotic partitioning of MCs and MBCs differs markedly (Ersfeld and Gull, 1997). During early mitosis, MCs leave the nuclear periphery and congregate as a rod-shaped clump positioned perpendicular to the central spindle. At anaphase, the MC clump splits into two equivalent-sized parts and each remains associated with the central spindle as they are pulled towards their respective poles. In contrast, at metaphase, MBCs are found outside the central spindle and, during anaphase, lag behind the MCs. Only at telophase are both MCs and MBCs present at the poles. These observations have led to the proposal that MCs do not need kinetochores to segregate; rather, they move along the central spindle at a ratio of several MCs per microtubule by an unknown mechanism, whereas MBC segregation relies on a conventional kinetochore-microtubule arrangement (Gull et al., 1998).

In the course of investigating *T. brucei* chromatin components, we identified *HTV* (histone H3 variant) and its corresponding protein H3V. Although sharing several features with those predicted for a CenH3, H3V localizes to telomeres and is not required for viability or chromosome segregation, indicating that it is a highly unusual variant of histone H3.

Materials and Methods

Strains and media

Bloodstream-form (strain Lister 427, antigenic type MITat 1.2, clone 221a) (Doyle et al., 1980) and procyclic trypanosomes were cultured in HMI-9 (Hirumi and Hirumi, 1989) or SDM-79 (Brun and Schonenberger, 1979), respectively. The bloodstream-form cell line 'single marker' and the procyclic-form (PF) cell line 29.13 both express T7 RNA polymerase and the Tet repressor, enabling the inducible expression of ectopic genes under control of the T7 promoter and Tet operator (Wirtz et al., 1999). Stable transfections and differentiations were performed as described (Wirtz et al., 1994; Overath et al., 1986).

Cloning histone genes

To clone *HTV*, a region corresponding to the partial cDNA clone AA694665 was PCR amplified from genomic DNA and ligated into pBluescript II SK$^+$, generating pJEL11. The pJEL11 insert was then used to probe a genomic Southern blot. The presence of a *Pst*I polymorphism upstream of the ORF meant that the *HTV* alleles could be distinguished as ~1.3 kb or ~1.8 kb fragments. The pJEL11 *HTV* insert was next used to probe a bacterial artificial chromosome (BAC) library derived from the Lister 427 strain (Zeng et al., 2001). BACs containing *HTV* were digested with *Pst*I, and the resulting DNA fragments were cloned into pBluescript II SK$^+$ and screened by PCR or colony blotting. pJEL32 and pJEL28 contain ~1.3 kbp or ~1.8 kbp *Pst*I *HTV* alleles respectively, which were sequenced and submitted to GenBank (Accession numbers AY179216 and AY179217).

Multiple ORFs corresponding to *HHT* (histone H3 gene) were sequenced as part of the *T. brucei* genome project (http://www.sanger.ac.uk/Projects/T_brucei/). Specific primers containing *Hin*dIII and *Bam*HI restriction sites were used to PCR amplify the complete *HHT* ORF from genomic DNA. This product was then digested with *Hin*dIII and *Bam*HI, cloned into pBluescript II SK$^+$ and sequenced to generate pJEL19.

Generation of tagged and fusion proteins

An endogenous *HTV* allele was tagged with the ten amino acid (EVHTNQDPLD) TY1 epitope (Bastin et al., 1996) by PCR amplifying the *phleo*/BB2 cassette (Shen et al., 2001) flanked by ~45 bp tracts of DNA corresponding to the regions immediately upstream and within the *HTV* allele and using this PCR product to transform the 29.13 cell line. A clonal cell line (PFJEL12) constitutively expressing TY1-H3V was identified.

Fusion between H3V and yellow fluorescent protein (YFP) was generated by amplifying *HTV* from pJEL32 by PCR using primers that eliminated the stop codon and introduced *Bam*HI sites at both ends of the molecule. The resulting fragment was digested with *Bam*HI and cloned into pJEL61, a variation of pLEW82 (Wirtz et al., 1999) in which the luciferase gene was replaced with YFP, generating pJEL73. An identical strategy was used to make an inducible construct that expressed H3-YFP except pJEL19 was used as a template; the resulting plasmid was named pJEL86. Sequencing confirmed that mutations had not been introduced into the coding regions of either *HTV* or *HHT* during PCR. pJEL73 and pJEL86 were linearized with *Not*I and stably introduced into precyclic-form cell line 29.13 to generate PFJEL4 and PFJEL7 respectively. Expression of H3V-YFP and H3-YFP was confirmed by western blotting.

Direct and indirect fluorescence microscopy and in situ hybridization

PFJEL4, expressing H3V-YFP, was grown to mid-log phase in the absence of tetracycline, washed in PBS, and settled onto aminopropyltriethoxysilane-coated coverslips. Immobilized cells were fixed for 10 minutes with 3.7% formaldehyde in PBS, permeabilized with 0.1% NP-40 for 5 minutes, blocked with PBG [PBS containing 0.2% cold fish gelatin (Sigma) and 0.5% BSA] and incubated with anti-β-tubulin mAb KMX (gift of K. Gull) for 1 hour. Subsequently, coverslips were incubated with TRITC-conjugated anti-mouse antibodies (Jackson ImmunoResearch Laboratories) for 1-2 hours, stained with DAPI and mounted in anti-fade solution.

A similar procedure was used to examine the localization of H3-YFP and TY1-H3V, except that washed PFJEL7 or PFJEL12 cells were fixed in solution with 2% formaldehyde in PBS for 10 minutes at 4°C and attached to coverslips by gentle centrifugation (5 minutes at ~600 ***g*** at 4°C). To detect the TY1 epitope, PFJEL12 coverslips were incubated with BB2 mAb (gift of K. Gull) for 1-2 hours, followed by secondary antibody as above.

For experiments in which the localization of TY1-H3V was combined with the detection of telomeric or 177-bp repeats by FISH, PFJEL12 cells were subject to immunofluorescence and then post-fixed with 3% formaldehyde in PBS for 5-10 minutes. FISH was subsequently carried out as described (Tan et al., 2002) using one of the following probes: TEL, a digoxigenin-labeled $(CCCUAA)_{27}$ RNA probe (Munoz-Jordan and Cross, 2001); MC177, a biotin-dUTP labeled mini-chromosome 177-bp repeat DNA probe (Ersfeld and Gull, 1997). The TEL probe was detected with sheep α-digoxigenin Fab fragment (Roche) and rhodamine conjugated α-sheep IgG (Jackson Laboratories). The MC177 probe was detected using Cy-3-conjugated ExtraAvidin (Sigma).

Except where noted, vertical stacks of 15-20 images (0.2 μm steps) were captured using DeltaVision (Applied Precision) deconvolution (softWoRx^{TM} v3.0 Software) microscopy and a subset were pseudo-colored and merged in Adobe Photoshop.

Chromatin immunoprecipitation (ChIP)

ChIP was carried out essentially as described (Loayza and De Lange, 2003), but with several modifications. ~4×10^8 procyclic cells were fixed for 10 minutes in 1% formaldehyde in SDM medium. Cells were combined with glycine (0.125 M final concentration) to stop the fixation and were subsequently washed with cold PBS, lysed and sonicated such that the resulting chromatin fragments averaged ~500 bp in length. Lysate was diluted with immunoprecipitation dilution buffer, pre-cleared by incubation with protein G agarose beads (Sigma) for 30 minutes, combined with either αGFP (Molecular Probes, A-11122) or αVSG117 (Hoek et al., 1999), incubated overnight at 4°C with rotation, supplemented with protein G agarose beads and finally incubated for a further ~2 hours. Immunoprecipitated material was washed, the chromatin eluted, the crosslinks reversed, and the DNA extracted and ethanol precipitated. The precipitate was resuspended in water, denatured with NaOH, and applied to Hybond N^+ membrane (Amersham) via a slot-blot apparatus. To compare the amount of material immunoprecipitated to the total input DNA, extracted DNA equivalent to 10% of each cell lysate input was included on the slot blot.

Hybridization of slot blots was carried out at 65°C using QuikHyb (Stratagene) supplemented with salmon sperm DNA. [α-^{32}P]dCTP labeled telomeric (TEL), mini-chromosome 177-bp repeat (MC177), and 5SDNA probes were generated using a Prime-It II labeling kit (Stratagene). The TEL probe corresponds to 800 bp of TTAGGG repeats (de Lange et al., 1990) whereas the MC177 and 5SDNA template DNA were generated by PCR amplification of genomic DNA as described (Ersfeld and Gull, 1997). Washes were performed as recommended by the manufacturer. Blots were exposed to a PhosphorImager screen and the percentage of the DNA precipitated was determined using ImageQuant software.

Generation of *htvΔ/htvΔ* cell lines

The constructs used to generate *htv* deletion mutants consisted of drug resistance cassettes flanked by DNA immediately adjacent to the *HTV* ORF. The hygromycin phosphotransferase ORF was PCR amplified and subcloned into *Bgl*II-digested pJEL37, a plasmid containing 300-400 bp of the regions immediately proximal to the *HTV* ORF separated by a *Bgl*II restriction site, to produce pJEL38. Additionally, the puromycin *N*-acetyltransferase ORF flanked by 5′ and 3′ splicing signals from the aldolase locus was released from pHD309 by digestion with *Sma*I and *Xho*I, blunted by treatment with Klenow fragment, and subcloned into pJEL37 that had been digested with *Bgl*II and blunted with Klenow, generating pJEL76. Knock-out cassettes were released from the vector backbone by restriction enzyme digestion and used to transform the 'single marker' cell line to produce BFJEL25. The absence of *HTV* alleles was confirmed by genomic Southern blotting.

Silencing assay

A *GFP* reporter was integrated into the active VSG221 expression site in 'single marker' and BFJEL25 by transfection with either CJ19 or CJ20 (gifts of C. Janzen) that had been linearized by digestion with *Bsm*I, resulting in the production of BFJEL36-BFJEL39. CJ20 is a modified version of pMig39 (Navarro et al., 1999), in which *GFP* has replaced luciferase; CJ19 is identical to CJ20 except the T7 promoter upstream of the *GFP* cassette has been deleted. After confirming that the transformants continued to express VSG221 and that constructs had integrated upstream of *VSG221*, cells were examined by flow cytometry to examine levels of GFP expression. Cell lines were then differentiated to procyclic form and examined for GFP expression again after 24 hours, 7, 10 and 14 days.

Results

A variant form of histone H3 is present in *T. brucei*

To identify variant forms of histone H3 in *T. brucei*, we searched public sequence databases for proteins sharing sequence similarity with major H3. We found a single cDNA containing a partial ORF that was predicted to encode a polypeptide meeting this criterion. Southern blotting showed that it corresponded to a single-copy gene (i.e. two copies in the diploid *T. brucei*) (data not shown), in contrast to histone H3, for which there are at least seven copies per haploid equivalent (Hall et al., 2003). Northern blotting confirmed that this gene was expressed in both bloodstream and procyclic forms (data not shown). Based on its sequence similarity with histone H3, we named this gene *HTV* (*H*istone H *T*hree *V*ariant) and its corresponding protein H3V (Fig. 1).

To obtain the complete sequence of *HTV*, we cloned and sequenced both alleles from a BAC library derived from the Lister 427 strain (see Materials and Methods). Although the two 420-bp ORFs differed slightly from one another, they are predicted to encode identical ~16 kDa proteins. H3V shares 45-62% sequence identity with major H3 from *T. brucei* and selected organisms (Fig. 1A); notably, the regions of extensive identity are confined to the C-terminal two-thirds of the protein.

We considered the possibility that H3V might be a *T. brucei* CenH3 (Fig. 1B). Although lacking a unique, conserved sequence motif, a typical CenH3 shares ~50-60% sequence identity with H3 within the histone fold domain, but has a highly divergent N-terminus, much like the situation for H3V. Additionally, a conserved glutamine residue in α1 helix of H3 is often absent in CenH3 and is likewise absent in H3V (see asterisk, Fig. 1A). However, in all CenH3s described to date, loop 1 is at least one and often several residues longer than the corresponding loop 1 within histone H3 (Henikoff et al., 2001). No such insertion exists in loop 1 of H3V (Fig. 1A,B). Thus, whereas the overall layout of H3V shares similarity with that expected for a CenH3, it does not meet the necessary sequence criteria to be declared a putative CenH3.

Variant forms of histone H3 also exist within the kinetoplast family (Fig. 1A). Although H3 from *Trypanosoma cruzi* and *Leishmania major* share ~90% and ~80% sequence identity respectively with H3 from *T. brucei* (data not shown), TcH3V and LmH3V share a more modest ~66% and ~50% sequence identity respectively with TbH3V. Like TbH3V, both LmH3V and TcH3V have divergent N-termini relative to their corresponding major histone H3, lack the conserved glutamine within α1 helix, and do not have an insertion in loop 1. These observations suggest that a variant H3 is conserved among kinetoplastids.

The sub-nuclear localization of H3V shifts over the course of the cell cycle

The major histones of *T. brucei* including H3 are distributed throughout the nucleus over the course of the cell cycle (see Fig. S1 in supplementary material) (our unpublished

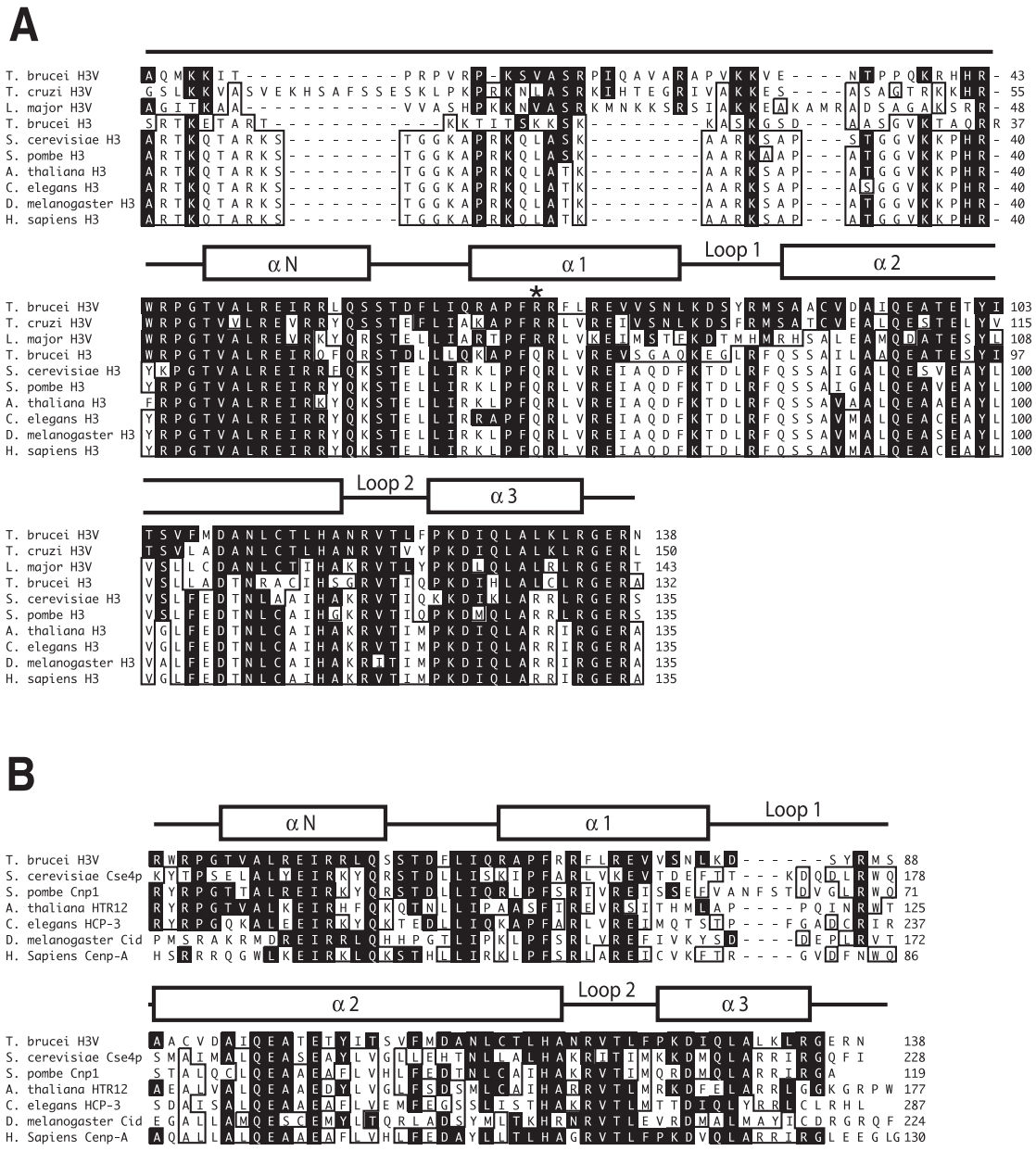

Fig. 1. *HTV* encodes a variant of histone H3. (A) The sequence of H3V aligned with variant forms of histone H3 from *T. cruzi* (http://TcruziDB.org) and *L. major* (Q9U196) and major histone H3 from *T. brucei* (Q810K5), *S. cerevisiae* (P02303), *S. pombe* (P09988), *Arabidopsis thaliana* (P59226), *C. elegans* (P08898), *Drosophila melanogaster* (P02299) and *Homo sapiens* (P16106). Amino acids conserved between H3V and other proteins are highlighted in black; boxed regions reveal identity among all proteins except H3V. An asterisk marks the site of a glutamine residue that is conserved in histone H3 but is often absent in CenH3s. (B) The primary structure of the histone-fold domain of H3V compared to Cse4p from *S. cerevisiae* (P36012), Cnp1 from *S. pombe* (Q9Y812), HTR12 from *A. thaliana* (AAL86775), Hcp-3 from *C. elegans* (CAA80160), Cid from *D. melanogaster* (AF259371) and Cenp-A from *H. sapiens* (P49450). Amino acids conserved between H3V and CenH3s are highlighted in black whereas those only conserved among CenH3s are boxed. Regions identified as corresponding to the helices αN, α1 and α2, and loop 1 and 2 are based on the crystal structure of histone H3 (Luger et al., 1997).

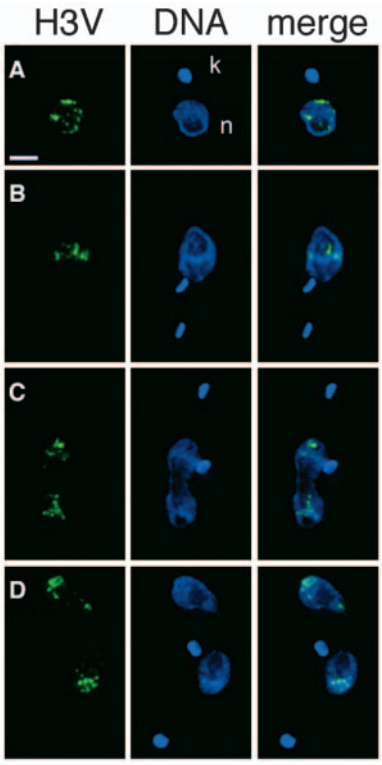

Fig. 2. The localization of H3V shifts dramatically over the cell cycle. A procyclic-form cell line (PFJEL12) expressing TY1-H3V (green) from its endogenous locus was subjected to indirect immunofluorescence, stained with DAPI to detect DNA (blue) and examined by deconvolution microscopy. (A) In interphase cells, TY1-H3V is often present as discrete foci at the nuclear periphery. (B) As the cell enters mitosis, TY1-H3V moves to the center of the nucleus. (C) As mitosis proceeds, TY1-H3V heads towards the poles. (D) At the end of mitosis, TY1-H3V remains at the poles before dispersing along the nuclear periphery. The region within the nucleus that is not stained by DAPI corresponds to the nucleolus as verified previously (Das et al., 1998). n, nucleus; k, kinetoplast. Bar, 2 μm.

observations). To examine the localization of H3V, we replaced one of the endogenous *HTV* alleles in procyclic-form cells with an allele encoding H3V fused at its N-terminus with the TY1 peptide tag (see Materials and Methods). As this allele was under the control of its endogenous promoter, we expected that the level of TY1-H3V would be similar to that found in wild-type cells. Upon confirmation by western blotting that a protein of the expected size was expressed (data not shown), the localization of TY1-H3V was examined over the course of the cell cycle by indirect immunofluorescence (Fig. 2).

In *T. brucei*, the mitochondrial DNA, known as the kinetoplast, completes its synthesis and division prior to mitosis (Woodward and Gull, 1990). Thus, by comparing the number of kinetoplasts (k) relative to nuclei (n), it is possible to monitor at which stage a particular cell is within the cell cycle. In interphase cells (1k 1n), numerous, distinct foci corresponding to TY1-H3V were present, often around the nuclear periphery (Fig. 2A). Intriguingly, TY1-H3V localization shifted dramatically as cells continued through the cell cycle (Fig. 2B-D). For example, in cells in early mitosis (two kinetoplasts and a single, diamond shaped nucleus), the majority of the TY1-H3V coalesced into a rod-shaped focus traversing the center of the nucleus (Fig. 2B). As the cell reached the later stages of mitosis, the TY1-H3V appeared to divide predominantly into two parts, each heading towards opposite ends of the dividing nucleus. In some cases, additional, smaller foci could be observed lagging behind the more intense clumps (Fig. 2C). Upon completion of nuclear division but prior to completion of cytokinesis, the majority of H3V remained present at the poles (Fig. 2D), and eventually became dispersed along the nuclear periphery (data not shown).

Comparable results were observed in bloodstream-form clones expressing TY-H3V (data not shown), indicating that the localization of H3V is independent of life cycle stage. Additionally, procyclic-form and bloodstream-form cell lines were generated that expressed either ectopic FLAG-H3V (the FLAG-epitope fused to the N-terminus of H3V) or H3V-YFP (yellow fluorescent protein fused to the C-terminus of H3V); all of these cell lines exhibited similar localization patterns (Fig. 3 and data not shown), indicating that the sub-nuclear localization of H3V was independent of its fusion partner.

H3V associates with the mitotic spindle and mini-chromosomes

The above observations suggested that H3V associates with either a specific class of chromosomes or a domain contained within many chromosomes. This hypothesis was supported by the finding that H3V associated with the mitotic spindle (Fig. 3). Spindle microtubules of procyclic-form cells were detected with an antibody (KMX) that recognized β-tubulin. In metaphase, H3V-YFP aligned perpendicular to the spindle (Fig. 3B), whereas in late mitotic cells, H3V-YFP was clearly distributed along the elongating closed (Fig. 3C) and bifurcated (Fig. 3D) spindle.

The H3V localization pattern and its association with the mitotic spindle bore striking similarity to that described previously for MCs (Ersfeld and Gull, 1997), and led us to speculate that H3V might be a component of MC chromatin. To address this question, we tested whether H3V colocalized with the 177-bp repeats (MC177), a repetitive DNA element which comprises ~90% of the mini-chromosome (Weiden et al., 1991), through a combination of indirect immunofluorescence and fluorescence in situ hybridization (FISH). As reported previously (Ersfeld and Gull, 1997), in interphase, many foci could be detected using the MC177 probe (Fig. 4A). In early mitotic cells, the MCs were present in the middle of the dividing nucleus (Fig. 4B). As the nucleus continued to divide, MCs were split and brought to opposite poles. During this process, much of the H3V signal either overlapped or abutted the MC177 signal (Fig. 4A-D). Often, however, some foci of H3V were detected that did not colocalize with MC177. This was particularly evident in late mitotic cells, in which trailing foci of H3V were observed (see arrowheads, Fig. 4C,D). Comparable results were observed in cell lines expressing H3V-YFP (data not shown). Thus, these experiments indicate that H3V associates with MCs, although the signal is not always coincident, suggesting it may not overlap with the 177-bp repeats themselves.

H3V colocalizes with telomeres

MCs, like MBCs, are capped with ~10-20 kbp of TTAGGG telomeric repeats (Munoz-Jordan et al., 2001). Given the small size of MCs, when dual FISH is performed with 177-bp repeat

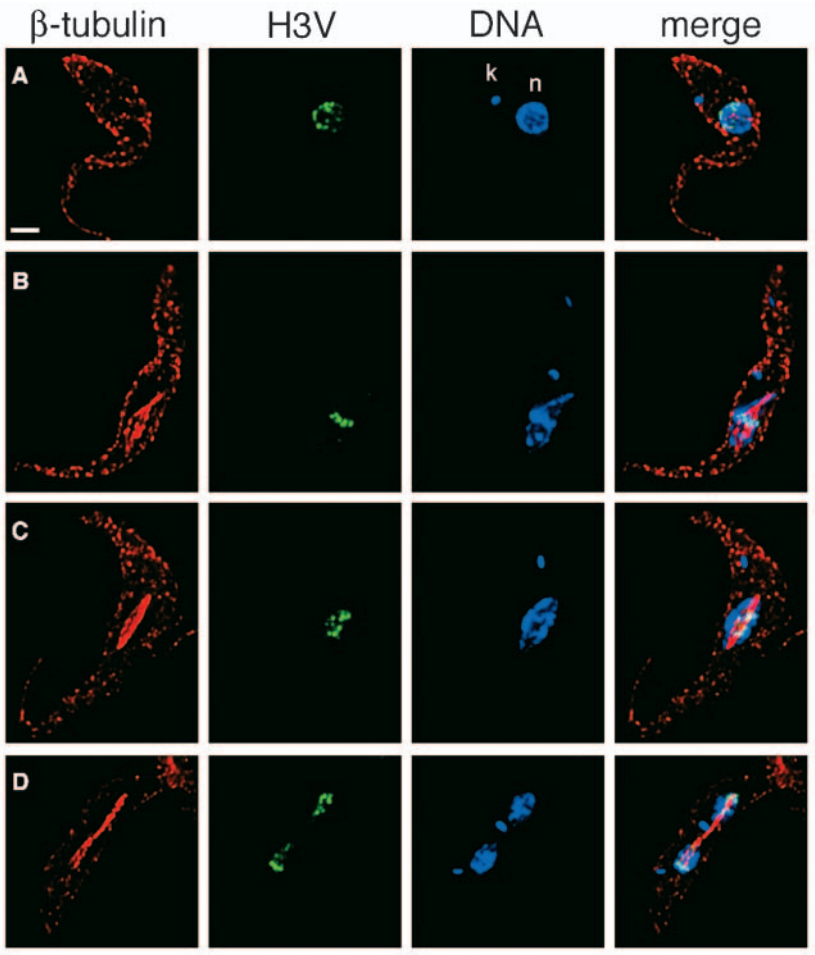

Fig. 3. H3V associates with the spindle during mitosis. (A-D) PFJEL4, a cell line expressing H3V-YFP (green), was fixed and stained with an antibody that recognizes β-tubulin (red). This antibody detects both the cytoskeleton and the mitotic spindle, and thus the outline of each cell is seen. DNA (blue) was visualized with DAPI. (A) At interphase, no spindle is observed and H3V-YFP is predominantly at the nuclear periphery. (B) In early mitosis, the spindle is visualized and H3V-YFP appears arrayed across it. (C,D) H3V-YFP continues its association with the spindle as it is pulled toward the poles. Bar, 2 μm.

and telomere specific probes, the two signals cannot be fully resolved (Ogbadoyi et al., 2000). Moreover, as there are many more MCs than MBCs, when FISH is carried out with a telomere-specific probe, the overall pattern of telomere localization is very similar to that of the 177-bp repeats. Foci corresponding to the telomeres of MBCs are most apparent during the late stages of the cell cycle, at which time they trail behind the MCs owing to their different partitioning mechanisms (Ersfeld and Gull, 1997). To determine whether H3V localizes to telomeres, we again combined immunofluorescence of endogenous TY1-H3V with FISH, this time using a probe specific for telomeric repeats (TEL). Although clearly not entirely coincident, much of the H3V signal overlapped that of the telomeric repeats (Fig. 5). This was true even during late mitosis, the stage at which MBCs can be distinguished from MCs because they are slower to reach the poles (Ersfeld and Gull, 1997). In some but not all instances, H3V signal was coincident with foci of telomeric signal that probably corresponded to MBCs (Fig. 5D, arrowheads). Similar results were observed in cell lines expressing H3V-YFP (data not shown).

H3V is enriched at telomeres

The observation that H3V colocalized with telomeres suggested it might be a component of telomeric chromatin. To test if H3V bound telomeric DNA, we performed chromatin immunoprecipitation (ChIP) analysis. Formaldehyde-cross-linked chromatin from a cell line expressing H3V-YFP was sheared and immunoprecipitated using an αGFP antibody that recognized YFP, or, as a non-specific antibody control, αVSG117. As additional controls, ChIP was carried out with wild-type cells and with cells expressing H3-YFP. Immunoprecipitated DNA was then examined by slot-blot for the presence of telomeric repeats or, as controls, 177-bp and 5S DNA repeats (Fig. 6A). No telomeric, 177-bp, or 5S DNA repeats were immunoprecipitated in a wild-type cell line, whereas all three types of repeats were present in the immunoprecipitated material in a cell line expressing H3-YFP, as would be expected given its distribution throughout the nucleus. A robust signal corresponding to the telomeric repeats was observed in the cell line expressing H3V-YFP, whereas only small amounts of 177-bp repeats and 5S DNA were detected in the immunoprecipitated material. No material was immunoprecipitated in the wild-type strain or when a non-specific antibody was used. Moreover, the immunoprecipitation of telomeric repeats did not occur in the absence of cross-linking reagent, indicating that the association reflects the situation in vivo and did not occur artificially during the ChIP procedure (data not shown).

Because slot blot analysis was used in the ChIP procedure, it was possible to directly quantify the percentage of a particular repeat that was immunoprecipitated relative to the total input (Fig. 6B). A comparison reveals that around twofold more telomeric repeats were immunoprecipitated with H3V-YFP than with H3-YFP (Fig. 6C). In contrast, H3V-YFP was inefficient at immunoprecipitating 177-bp repeats and 5S DNA compared to H3-YFP (Fig. 6C). Thus, H3V is enriched at telomeres relative to other repetitive DNA sequences.

HTV is not essential for viability

To test if *HTV* is an essential gene, we exchanged both endogenous alleles in a bloodstream-form cell line with 'knock-out' cassettes conferring resistance to hygromycin or puromycin. We generated multiple, independent clones and, by Southern blotting, confirmed that both alleles of the *HTV* ORF were deleted (data not shown). *htvΔ/htvΔ* bloodstream-form strains grew indistinguishably from the wild type, had no gross defects in the cell cycle and remained competent to infect mice (data not shown). Additionally, *htvΔ/htvΔ* mutants were able to differentiate to the procyclic stage, indicating that *HTV* is also not essential for viability in this stage of the life cycle (data not shown).

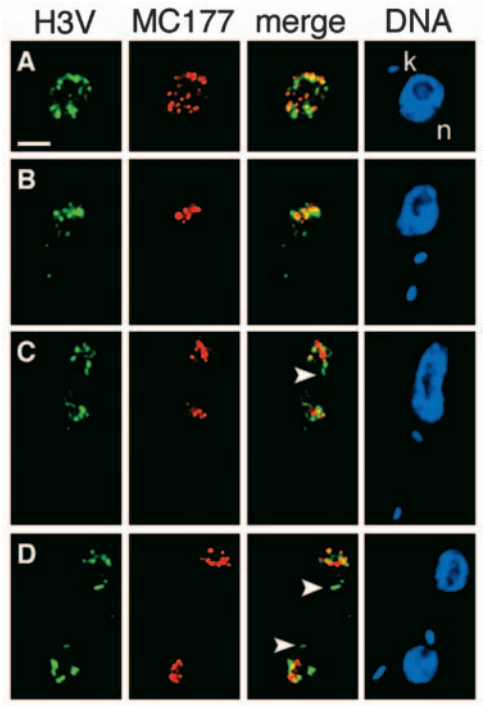

Fig. 4. H3V associates with mini-chromosomes. (A-D) Indirect-immunofluorescence of TY1-H3V (green) was combined with detection of mini-chromosomes by FISH using a probe specific for the 177-bp repeats (MC177, red). DNA (blue) was detected with DAPI. All cells are procyclics (PFJEL12) at (A) interphase, (B,C) mitosis and (D) late mitosis. Arrowheads indicate trailing TY1-H3V foci that do not overlap with 177-bp repeats. Bar, 2 μm.

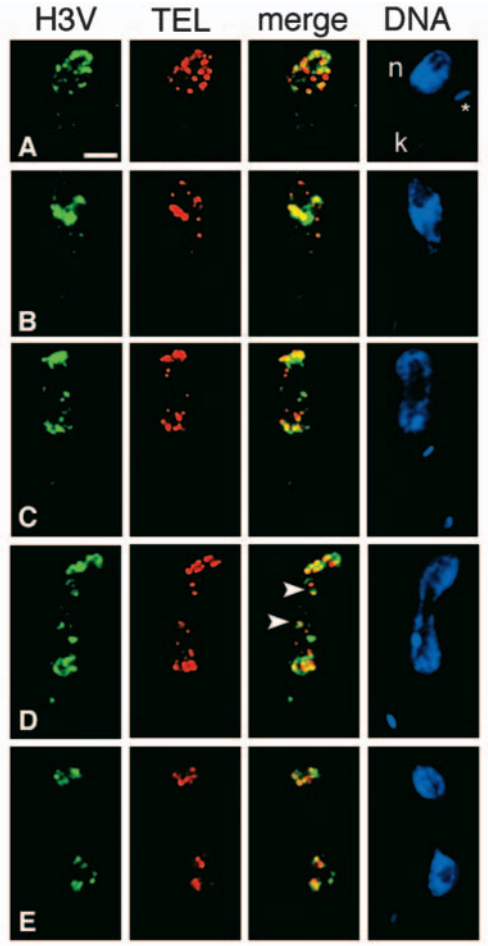

Fig. 5. H3V colocalizes with telomeres. (A-E) Indirect immunofluorescence of TY1-H3V (green) was combined with FISH using a probe specific for the telomeric TTAGGG repeats (TEL, red) found at the ends of all chromosomes. DNA (blue) was detected with DAPI stain. All cells are procyclics (PFJEL12) at (A) interphase, (B,C) mitosis, (D) late mitosis and (E) karyokinesis. Arrowheads indicate TY1-H3V foci that are coincident with telomeric foci that may correspond to MBCs. Asterisk indicates a kinetoplast of an adjacent cell. Bar, 2 μm.

Our observations that H3V localized to telomeres but was not required for viability, led us to search for telomere-associated phenotypes in *htvΔ/htvΔ* mutants. Telomere restriction fragment analysis of *htvΔ/htvΔ* mutants revealed that telomeres continued to elongate in a manner similar to wild-type cells (Bernards et al., 1983), indicating that loss of *HTV* does not impede telomere maintenance (data not shown). We considered the possibility that absence of H3V might affect MC stability and that such a phenotype could require many generations to be clearly manifested. First, by slot blot analysis of total genomic DNA hybridized to the MC177 and TEL probes, we directly compared the amount of 177-bp repeats (as a measurement of mini-chromosomes) and telomeric repeats present in wild-type cells versus those in *htvΔ/htvΔ* mutants grown continuously for ~2 months (~220 cell divisions). No differences were noted between strains (data not shown). Second, over the course of ~7.5 months (>800 cell divisions), we periodically examined the distribution of MC and telomere foci in *htvΔ/htvΔ* mutants by FISH using the MC177 and TEL probes. Again, no changes were detected (data not shown).

htv/htv mutants retain the ability to 'silence' expression sites

Antigenic variation in *T. brucei* is controlled by telomere-proximal expression sites (Borst and Ulbert, 2001). As our results indicated that H3V is enriched at telomeres and that telomeric chromatin may influence transcription at expression sites (Horn and Cross, 1995; Navarro et al., 1999), we asked if the transcription of expression site-linked *VSGs* was affected in *htvΔ/htvΔ* bloodstream-form and procyclic-form mutants. In a wild-type bloodstream form cell line, cells express VSG221, switching to another VSG only infrequently (10^{-5}-10^{-6}) (Horn and Cross, 1997a). *htvΔ/htvΔ* mutants continued to express VSG221 as revealed by indirect immunofluorescence with an antibody to VSG221 (data not shown). To test if additional VSGs were expressed, we prepared cDNA from wild-type cells and *htvΔ/htvΔ* mutants and, by real-time PCR, tested for the presence of *VSG221* cDNA as well as several other telomere proximal, expression site-linked *VSGs* (*bR2*, *B*, *VO2*) that are ordinarily in the 'off' state. We observed a robust PCR product corresponding to *VSG221* in both wild-type cells and *htvΔ/htvΔ* mutants (~1400 mRNA copies/cell and ~1600 mRNA copies/cell, respectively) (data not shown). In contrast, in wild-type cells, we were unable to detect *VSGB* and could detect *VSGbR2* and *VSGVO2* at only extremely low levels (<1

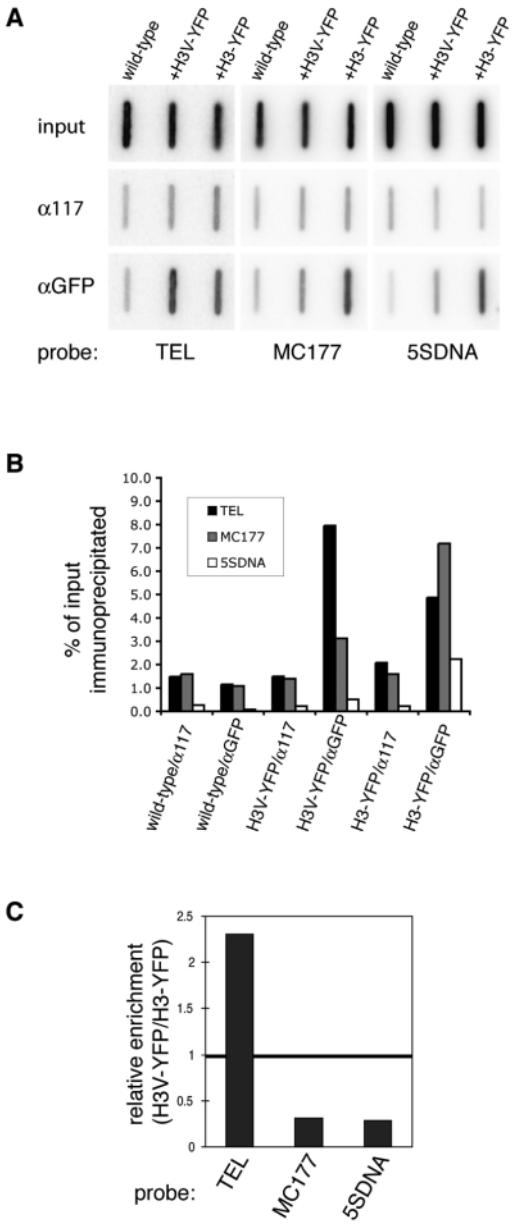

Fig. 6. H3V is enriched at telomeres. (A) Chromatin immunoprecipitation was carried out on procyclic wild-type cells (29.13) or cells expressing H3V-YFP (PFJEL4) or H3-YFP (PFJEL7). In each series, chromatin was immunoprecipitated with either a non-specific (α117) or a specific antibody (αGFP). Immunoprecipitated DNA was analyzed by slot blots hybridized with probes specific for telomeric repeats (TEL), mini-chromosome 177-bp repeats (MC177), or 5SDNA. Note that the input control corresponds to 10% of total. ChIPs were performed two to four times and a representative slot blot is shown for each set. (B) A quantitative presentation of the data shown in A and from one to three other independent experiments reveals the average percentage of input material present in control (α117) and test (αGFP) ChIPs. (C) Relative to major H3, H3V is enriched at telomeres and is found at reduced levels at two other genomic loci. To determine these ratios, the background signal value (i.e. the material immunoprecipitated by the non-specific antibody) was subtracted from αGFP signal value to generate a specific signal value; the specific signal value of H3V-YFP divided by the specific signal value of H3-YFP equals the relative enrichment.

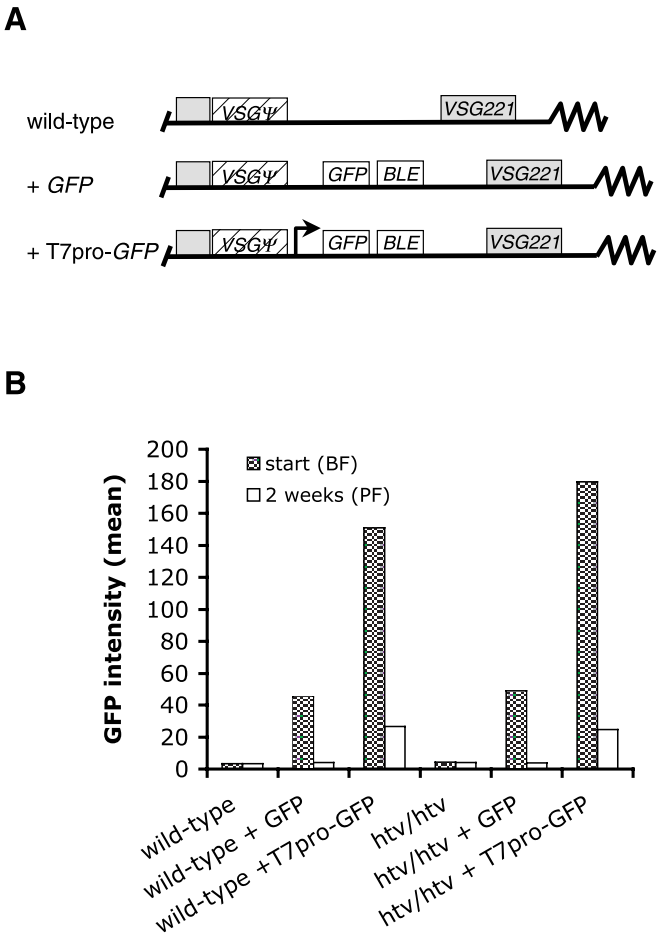

Fig. 7. Silencing of an expression site upon differentiation to the procyclic form is unaffected by loss of H3V. (A) Schematic diagram of telomere (zig-zag) proximal portion of the *221* expression site and the *221* expression site in which either *GFP-BLE* cassette or T7 promoter driven *GFP-BLE* was inserted. (B) Comparison of the GFP fluorescence intensity from the wild type (single marker), wild type + *GFP* (BFJEL36), wild type + *T7-GFP* (BFJEL37) and *htvΔ/htvΔ* (BFJEL25), *htvΔ/htvΔ* + *GFP* (BFJEL38) and *htvΔ/htvΔ* + *T7-GFP* (BFJEL39) bloodstream-form cell lines and the same cell lines following two weeks differentiation to the procyclic form.

mRNA copy/cell). Importantly, these levels were unchanged in the mutants (data not shown), indicating that other expression sites had not lost their ability to silence *VSG* in the absence of H3V. *VSG221* could be detected in mixing experiments in which wild-type bloodstream-form cells were combined with procyclic form at ratios of 1:100-1:10,000, suggesting that had any of the normally silenced *VSGs* been activated to a modest degree, we should have detected them (data not shown).

To investigate the role of chromatin structure in expression site transcriptional regulation, we have established an assay to measure chromatin accessibility. A reporter gene under the control of the T7 promoter positioned at active or inactive expression sites could be transcribed by ectopic T7 RNA polymerase in bloodstream-form cells (Navarro et al., 1999). Upon differentiation to the procyclic form, however, T7 polymerase-driven transcription of the reporter gene was reduced ~100-fold. This finding suggests that the chromatin at

expression sites in procyclic-form cells is no longer accessible to T7 polymerase (Navarro et al., 1999). We tested whether loss of H3V could trigger a change at expression sites that would allow T7 polymerase to access the T7 promoter in procyclic-form cells. To this end, a T7 promoter driven GFP reporter construct was inserted in the active 221 expression site between *VSG221* and a unique upstream *VSG* pseudogene in either bloodstream-form wild-type cells or an *htvΔ/htvΔ* mutant. To test if the active expression site could be silenced upon differentiation to the procyclic form, additional cell lines were constructed in which the GFP reporter lacked the T7 promoter (Fig. 7A). As expected, all cell lines initially expressed GFP as assessed by microscopy and by FACS. We note that intensity of GFP signal was increased in the presence of the T7 promoter. However, as cells were differentiated, both those lacking the T7 promoter and those containing it dramatically reduced expression of GFP regardless of whether or not *HTV* was present (Fig. 7B). We infer that bloodstream-form cells lacking H3V remain competent to shut down the active expression site upon differentiation to the procyclic form.

Discussion

A telomere-enriched variant of histone H3

Through a series of localization and colocalization experiments, we have demonstrated that H3V shifts throughout the cell cycle in a pattern closely resembling that of MCs and telomeres. ChIP analysis indicated that H3V was enriched at sites of telomeric repeat DNA, but at neither the mini-chromosomal 177-bp repeat nor the 5SDNA loci.

In human sperm, a variant form of histone H2B associates specifically with telomeric DNA in vitro, but colocalizes with only a subset of telomeres (Gineitis et al., 2000). In contrast, our data are consistent with the presence of H3V at the telomeres of all classes of chromosomes. Because of the small size of MCs, the 177-bp repeat and telomere-specific signals cannot be fully resolved (Ogbadoyi et al., 2000). When H3 localization was combined with MC177 FISH, we observed that H3V signal overlapped that of the MC177 probe. This observation combined with the finding that telomeric repeats, but not 177-bp repeats, are immunoprecipitated by H3V is consistent with H3V being present at MC telomeres. H3V association with MBC telomeres is harder to visualize. Because there are many more MCs than MBCs within a nucleus, resolving these two classes of chromosomes is best achieved during mitosis, when MCs segregate more rapidly than MBCs (Ersfeld and Gull, 1997). During late mitosis, when H3V localization was combined with 177-bp repeat FISH, some H3V signal could be observed lagging behind the MCs, leading us to speculate that these foci of H3V were associated with MBCs. When H3V localization was combined with telomeric FISH, many of the lagging H3V foci colocalized with TEL probe, as would be expected if H3V were bound to the telomeres of MBCs. Our failure to detect complete colocalization between H3V and the TEL probe could be due to the technical difficulties in combining immunofluorescence with FISH. We have found that conditions where TEL FISH signal are optimized interfere with immunofluorescence of H3V and vice-versa. Alternatively, H3V may not be present at all telomeres and/or is present at loci in addition to telomeres.

In the ChIP procedure, chemically cross-linked DNA is sheared to ~500 bp prior to immunoprecipitation. Although the immunoprecipitated DNA clearly hybridized to a telomeric repeat probe, we cannot exclude the possibility that H3V associates with sub-telomeric DNA and that the telomeric repeats were immunoprecipitated by virtue of their proximity to sub-telomeric sequences. Interestingly, the sub-telomeric 29 bp repeats, found in multiple copies immediately proximal to the telomeres of mini-chromosomes, contain a telomere repeat-derived sequence including a single TTAGGG hexamer (Weiden et al., 1991). The simplest interpretation of our combined localization and ChIP data is that H3V-containing chromatin is enriched at or near telomeres of most, if not all, chromosome ends.

We note that the telomeric DNA repeat unit, but not the sub-telomeric sequences, are identical in *T. brucei*, *T. cruzi* and *L. major* (Wickstead et al., 2003). It will be interesting to test whether the variant forms of histone H3 that we identified by mining the *T. cruzi* and *L. major* sequence databases are also enriched at telomeres.

A telomeric function for H3V?

Telomeric chromatin typically exhibits heterochromatin-like properties. For instance, telomeres are late-replicating and have the ability to transcriptionally silence genes positioned nearby (reviewed by Tham and Zakian, 2002). Although specific TTAGGG repeat binding proteins have not been described in *T. brucei*, position-dependent telomeric silencing has been demonstrated, suggesting that the sub-telomeric location of expression sites may contribute to their transcriptional control in bloodstream-form cells (Horn and Cross, 1995; Horn and Cross, 1997b). Additionally, the transcriptional attenuation of expression site promoters that occurs when the bloodstream form differentiates to the procyclic form may involve changes in chromatin structure (Navarro et al., 1999).

The observation that H3V is enriched at telomeres suggested that it might function at telomeres. As assessed by micrococcal nuclease digestion, at least a portion of telomeric DNA in *T. brucei* is packaged in nucleosomes (our unpublished observations), presumably corresponding to more internal chromosome regions of the telomere, as has been observed in other organisms (Tommerup et al., 1994). Surprisingly, telomere-related phenotypes were not detected in *htvΔ/htvΔ* mutants: the elongation of telomeric DNA was not impaired, *VSG* silencing at inactive expression sites was maintained in bloodstream-form cells and the active expression site was repressed upon differentiation to the procyclic stage. We note, however, that the functions of histones are often at least partially redundant. For example, in *S. cerevisiae*, the N-termini of histones H3 and H4 are involved in the transcriptional silencing that occurs at the silent mating-type loci; however in the case of histone H3, its role was only revealed when combined with a mutation in a second chromatin component (Thompson et al., 1994). Thus, in *htvΔ/htvΔ* mutants, it is possible that another, functionally redundant protein could be taking its place. Moreover, if the phenotypes associated with loss of *HTV* were subtle, they may not have been detected in our assays. Alternatively, as has been suggested for the Sir2-4 proteins in *S. cerevisiae* (Tham and Zakian, 2002), telomeres may serve as a reservoir for H3V. When as yet unknown circumstances dictate, H3V could shift to relevant sites in the genome.

Is H3V the CenH3 of *T. brucei*?

In eukaryotes, the challenge of faithfully segregating replicated chromosomes is overcome, in part, by centromeres. Centromeres are attached to microtubules via kinetochores within the mitotic spindle, allowing chromosome pairs to be pulled apart. Centromeres, however, are not conserved in either sequence or size. For example, the point centromeres of *S. cerevisiae* consist of only ~125 bp of DNA containing three consensus elements, whereas those in plants and most animals are composed of long (kbp to Mbp) stretches of highly repetitive satellite DNA; in nematodes, by contrast, chromosomes are holocentric with microtubule attachment sites occurring along the length of the chromosome (reviewed by Tyler-Smith and Floridia, 2000). Despite the tremendous variation in centromeric DNA composition from one species to the next, all eukaryotes are thought to have a centromere-specific form of histone H3 (Henikoff et al., 2001). When we began this work, the *T. brucei* genome sequencing project was in its nascent stage and no CenH3 candidates had been identified. Now that it is nearly complete and we have been unable to find additional variant forms of histone H3, we propose that H3V may be the sole variant form of histone H3 in *T. brucei*. If true, a re-evaluation of whether H3V could be the CenH3 of *T. brucei* is necessary.

In contrast to core histones, CenH3s are rapidly evolving proteins (Malik and Henikoff, 2001), sharing sequence similarity with each other and histone H3 only within the histone-fold domain, and are capped with N-termini that are diverse in both sequence and size. H3V, like a typical CenH3, shares ~57% sequence identity with its major histone H3 counterpart, and this region maps exclusively to the histone-fold domain. We have additionally identified variant forms of histone H3 in *T. cruzi* and *L. major*. Although we have no functional data about either of these proteins, TcH3V and LmH3V are probably orthologs of TbH3V. If true, it is interesting to note that variant forms of H3 from *T. brucei*, *T. cruzi* and *L. major* exhibit much greater sequence diversity (~50-66% sequence identity) than major H3 from these same organisms (80-90% sequence identity; data not shown). Nevertheless, the primary structure of these kinetoplast H3Vs lack a key hallmark of CenH3: an insertion in Loop 1, which has been found in all experimentally validated CenH3s (Henikoff et al., 2001).

The driving force underlying the diversity among CenH3s has been proposed to be the rapid evolution of the centromeric DNA sequences due, in part, to meiotic drive (Henikoff et al., 2001). For a cell to retain its complete chromosome complement during mitosis, CenH3 must successfully associate with the centromeric DNA present on each chromosome, which often contains little or no sequence conservation among chromosomes. In *T. brucei*, centromeric DNA has not been identified, although several candidates have been proposed. These include the 177-bp repeats present on MCs (Weiden et al., 1991), a ~5.5 kbp repetitive region within chromosome I (Hall et al., 2003) and unspecified sequences within a ~269 kbp recombinational 'cold region' on the right arm of chromosome II (El-Sayed et al., 2003). Frustratingly, no components of the kinetochore have been characterized either. Accordingly, testing whether H3V colocalizes with either centromeric DNA or kinetochores remains a tricky proposition.

Although we do not know if H3V is at centromeres, we have shown that it associates with the spindle during mitosis and is apparently present at most, if not all, telomeres. Although surprising, a telomeric localization should not immediately discount the possibility that H3V could be a CenH3 because, in fact, telomeres and sub-telomeric regions have been linked to centromere function. During meiosis in the nematode *Parascaris univalens*, the heterochromatic ends of chromosomes interact with microtubules and provide centromere function (Goday and Pimpinelli, 1989). In *L. major*, chromosome fragmentation studies have implicated sub-telomeric regions in chromosome maintenance and stability, suggesting these satellite DNA rich regions have centromeric properties (Dubessay et al., 2002). If telomeres provide centromere function in *T. brucei*, we would predict that they would lead chromosomes towards the poles during mitosis, with more internal chromosome regions lagging behind. A combination of telomeric FISH and chromosome painting may allow this issue to be addressed for the MBCs.

Where tested, CenH3s have been shown to be required for chromosome segregation and to be essential for viability (Stoler et al., 1995; Takahashi et al., 2000; Sanyal and Carbon, 2002). Thus, the strongest argument that H3V is not the CenH3 of *T. brucei* stems from our observations that an *htvΔ/htvΔ* mutant is viable and has no gross defects in chromosome segregation in either bloodstream-form cells or newly differentiated procyclic-form cells. Within the tsetse, wild-type procyclic-form cells undergo further morphological and metabolic changes as they leave the mid-gut and make their way to the salivary glands, where they differentiate into metacyclic cells. Additionally, although poorly understood, *T. brucei* can undergo genetic exchange in the fly. Whether *htvΔ/htvΔ* mutants might reveal a CenH3-related phenotype or defects in genetic exchange when passaged through the tsetse fly, however, has not yet been tested.

We thank Klaus Ersfeld and Keith Gull for numerous reagents and advice, András Fiser and Andrej Sali for modeling the structures of *T. brucei* histones, Juliano Timm and Fabian Lander for help with real-time PCR, Christian Janzen for assistance with silencing assays, and members of the Cross lab for discussions and critical reading of this manuscript. Microscopy was carried out at the RU Bio-Imaging Resource Center with guidance from Alison North. J.E.L. was supported by fellowships from the Charles H. Revson Foundation and the NIH (AI10380). This work was also supported by a grant to G.A.M.C. from the NIH (AI21729).

References

Ahmad, K. and Henikoff, S. (2002a). The histone variant H3.3 marks active chromatin by replication-independent nucleosome assembly. *Mol. Cell* **9**, 1191-1200.

Ahmad, K. and Henikoff, S. (2002b). Histone H3 variants specify modes of chromatin assembly. *Proc. Natl. Acad. Sci. USA* **99**, 16477-16484.

Bastin, P., Bagherzadeh, Z., Matthews, K. R. and Gull, K. (1996). A novel epitope tag system to study protein targeting and organelle biogenesis in *Trypanosoma brucei*. *Mol. Biochem. Parasitol.* **77**, 235-239.

Bender, K., Betschart, B., Schaller, J., Kampfer, U. and Hecker, H. (1992). Sequence differences between histones of procyclic *Trypanosoma brucei brucei* and higher eukaryotes. *Parasitology* **105**, 97-104.

Bernards, A., Michels, P. A., Lincke, C. R. and Borst, P. (1983). Growth of chromosome ends in multiplying trypanosomes. *Nature* **303**, 592-597.

Borst, P. and Ulbert, S. (2001). Control of VSG gene expression sites. *Mol. Biochem. Parasitol.* **114**, 17-27.

Brun, R. and Schonenberger, M. (1979). Cultivation and in vitro cloning of procyclic culture forms of *Trypanosoma brucei* in a semi-defined medium. *Acta Trop.* **36**, 289-292.

Cross, G. A. M. (1996). Antigenic variation in trypanosomes: secrets surface slowly. *Bioessays* **18**, 283-291.

Das, A., Park, J. H., Hagen, C. B. and Parsons, M. (1998). Distinct domains of a nucleolar protein mediate protein kinase binding, interaction with nucleic acids and nucleolar localization. *J. Cell Sci.* **111**, 2615-2623.

de Lange, T., Shiue, L., Myers, R. M., Cox, D. R., Naylor, S. L., Killery, A. M. and Varmus, H. E. (1990). Structure and variability of human chromosome ends. *Mol. Cell. Biol.* **10**, 518-527.

Doyle, J. J., Hirumi, H., Hirumi, K., Lupton, E. N. and Cross, G. A. M. (1980). Antigenic variation in clones of animal-infective *Trypanosoma brucei* derived and maintained in vitro. *Parasitology* **80**, 359-369.

Dubessay, P., Ravel, C., Bastien, P., Stuart, K., Dedet, J. P., Blaineau, C. and Pages, M. (2002). Mitotic stability of a coding DNA sequence-free version of *Leishmania major* chromosome 1 generated by targeted chromosome fragmentation. *Gene* **289**, 151-159.

El-Sayed, N. M., Ghedin, E., Song, J., MacLeod, A., Bringaud, F., Larkin, C., Wanless, D., Peterson, J., Hou, L., Taylor, S. et al. (2003). The sequence and analysis of *Trypanosoma brucei* chromosome II. *Nucleic Acids Res.* **31**, 4856-4863.

Ersfeld, K. and Gull, K. (1997). Partitioning of large and minichromosomes in *Trypanosoma brucei*. *Science* **276**, 611-614.

Ersfeld, K., Melville, S. E. and Gull, K. (1999). Nuclear and genome organization in *Trypanosoma brucei*. *Parasitology Today* **15**, 58-63.

Fischle, W., Wang, Y. and Allis, C. D. (2003a). Histone and chromatin cross-talk. *Curr. Opin. Cell Biol.* **15**, 172-183.

Fischle, W., Wang, Y. and Allis, C. D. (2003b). Binary switches and modification cassettes in histone biology and beyond. *Nature* **425**, 475-479.

Garcia-Salcedo, J. A., Gijon, P., Nolan, D. P., Tebabi, P. and Pays, E. (2003). A chromosomal SIR2 homologue with both histone NAD-dependent ADP-ribosyltransferase and deacetylase activities is involved in DNA repair in Trypanosoma brucei. *EMBO J.* **22**, 5851-5862.

Gineitis, A. A., Zalenskaya, I. A., Yau, P. M., Bradbury, E. M. and Zalensky, A. O. (2000). Human sperm telomere-binding complex involves histone H2B and secures telomere membrane attachment. *J. Cell Biol.* **151**, 1591-1598.

Goday, C. and Pimpinelli, S. (1989). Centromere organization in meiotic chromosomes of *Parascaris univalens*. *Chromosoma* **98**, 160-166.

Gull, K., Alsford, S. and Ersfeld, K. (1998). Segregation of minichromosomes in trypanosomes: implications for mitotic mechanisms. *Trends Microbiol.* **6**, 319-323.

Hall, N., Berriman, M., Lennard, N. J., Harris, B. R., Hertz-Fowler, C., Bart-Delabesse, E. N., Gerrard, C. S., Atkin, R. J., Barron, A. J., Bowman, S. et al. (2003). The DNA sequence of chromosome I of an African trypanosome: gene content, chromosome organisation, recombination and polymorphism. *Nucleic Acids Res.* **31**, 4864-4873.

Henikoff, S., Ahmad, K. and Malik, H. S. (2001). The centromere paradox: stable inheritance with rapidly evolving DNA. *Science* **293**, 1098-1102.

Hirumi, H. and Hirumi, K. (1989). Continuous cultivation of *Trypanosoma brucei* blood stream forms in a medium containing a low concentration of serum protein without feeder cell layers. *J. Parasitol.* **75**, 985-989.

Hoek, M., Xu, H. and Cross, G. A. M. (1999). *Trypanosoma brucei*: generation of specific antisera to recombinant variant surface glycoproteins. *Exp. Parasitol.* **91**, 199-202.

Horn, D. (2001). Nuclear gene transcription and chromatin in *Trypanosoma brucei*. *Int. J. Parasitol.* **31**, 1157-1165.

Horn, D. and Cross, G. A. M. (1995). A developmentally regulated position effect at a telomeric locus in *Trypanosoma brucei*. *Cell* **83**, 555-561.

Horn, D. and Cross, G. A. M. (1997a). Analysis of *Trypanosoma brucei* vsg expression site switching in vitro. *Mol. Biochem. Parasitol.* **84**, 189-201.

Horn, D. and Cross, G. A. M. (1997b). Position-dependent and promoter-specific regulation of gene expression in *Trypanosoma brucei*. *EMBO J.* **16**, 7422-7431.

Loayza, D. and de Lange, T. (2003). POT1 as a terminal transducer of TRF1 telomere length control. *Nature* **424**, 1013-1018.

Luger, K., Mader, A. W., Richmond, R. K., Sargent, D. F. and Richmond, T. J. (1997). Crystal structure of the nucleosome core particle at 2.8Å resolution. *Nature* **389**, 251-260.

Malik, H. S. and Henikoff, S. (2001). Adaptive evolution of Cid, a centromere-specific histone in Drosophila. *Genetics* **157**, 1293-1298.

Malik, H. S. and Henikoff, S. (2003). Phylogenomics of the nucleosome. *Nat. Struct. Biol.* **10**, 882-891.

Munoz-Jordan, J. L. and Cross, G. A. M. (2001). Telomere shortening and cell cycle arrest in *Trypanosoma brucei* expressing human telomeric repeat factor TRF1. *Mol. Biochem. Parasitol.* **114**, 169-181.

Munoz-Jordan, J. L., Cross, G. A. M., de Lange, T. and Griffith, J. D. (2001). t-loops at trypanosome telomeres. *EMBO J.* **20**, 579-588.

Navarro, M. and Gull, K. (2001). A pol I transcriptional body associated with VSG mono-allelic expression in *Trypanosoma brucei*. *Nature* **414**, 759-763.

Navarro, M., Cross, G. A. M. and Wirtz, E. (1999). *Trypanosoma brucei* variant surface glycoprotein regulation involves coupled activation/inactivation and chromatin remodeling of expression sites. *EMBO J.* **18**, 2265-2272.

Ogbadoyi, E., Ersfeld, K., Robinson, D., Sherwin, T. and Gull, K. (2000). Architecture of the *Trypanosoma brucei* nucleus during interphase and mitosis. *Chromosoma* **108**, 501-513.

Overath, P., Czichos, J. and Haas, C. (1986). The effect of citrate/cis-aconitate on oxidative metabolism during transformation of *Trypanosoma brucei*. *Eur. J. Biochem.* **160**, 175-182.

Roditi, I., Furger, A., Ruepp, S., Schurch, N. and Butikofer, P. (1998). Unravelling the procyclin coat of *Trypanosoma brucei*. *Mol. Biochem. Parasitol.* **91**, 117-130.

Sanyal, K. and Carbon, J. (2002). The CENP-A homolog CaCse4p in the pathogenic yeast *Candida albicans* is a centromere protein essential for chromosome transmission. *Proc. Natl. Acad. Sci. USA* **99**, 12969-12974.

Shen, S., Arhin, G. K., Ullu, E. and Tschudi, C. (2001). In vivo epitope tagging of *Trypanosoma brucei* genes using a one step PCR-based strategy. *Mol. Biochem. Parasitol.* **113**, 171-173.

Stevens, J. R., Noyes, H. A., Schofield, C. J. and Gibson, W. (2001). The molecular evolution of Trypanosomatidae. *Adv. Parasitol.* **48**, 1-56.

Stoler, S., Keith, K. C., Curnick, K. E. and Fitzgerald-Hayes, M. (1995). A mutation in CSE4, an essential gene encoding a novel chromatin-associated protein in yeast, causes chromosome nondisjunction and cell cycle arrest at mitosis. *Genes Dev.* **9**, 573-586.

Strahl, B. D. and Allis, C. D. (2000). The language of covalent histone modifications. *Nature* **403**, 41-45.

Takahashi, K., Chen, E. S. and Yanagida, M. (2000). Requirement of Mis6 centromere connector for localizing a CENP-A-like protein in fission yeast. *Science* **288**, 2215-2219.

Tan, K. S., Leal, S. T. and Cross, G. A. M. (2002). *Trypanosoma brucei* MRE11 is non-essential but influences growth, homologous recombination and DNA double-strand break repair. *Mol. Biochem. Parasitol.* **125**, 11-21.

Tham, W. H. and Zakian, V. A. (2002). Transcriptional silencing at Saccharomyces telomeres: implications for other organisms. *Oncogene* **21**, 512-521.

Thompson, J. S., Ling, X. and Grunstein, M. (1994). Histone H3 amino terminus is required for telomeric and silent mating locus repression in yeast. *Nature* **369**, 245-247.

Tommerup, H., Dousmanis, A. and de Lange, T. (1994). Unusual chromatin in human telomeres. *Mol. Cell. Biol.* **14**, 5777-5785.

Tyler-Smith, C. and Floridia, G. (2000). Many paths to the top of the mountain: diverse evolutionary solutions to centromere structure. *Cell* **102**, 5-8.

Weiden, M., Osheim, Y. N., Beyer, A. L. and van der Ploeg, L. H. (1991). Chromosome structure: DNA nucleotide sequence elements of a subset of the minichromosomes of the protozoan *Trypanosoma brucei*. *Mol. Cell. Biol.* **11**, 3823-3834.

Wickstead, B., Ersfeld, K. and Gull, K. (2003). Repetitive elements in genomes of parasitic protozoa. *Microbiol. Mol. Biol. Rev.* **67**, 360-375.

Wirtz, E., Hartmann, C. and Clayton, C. (1994). Gene expression mediated by bacteriophage T3 and T7 RNA polymerases in transgenic trypanosomes. *Nucleic Acids Res.* **22**, 3887-3894.

Wirtz, E., Leal, S., Ochatt, C. and Cross, G. A. M. (1999). A tightly regulated inducible expression system for conditional gene knock-outs and dominant-negative genetics in *Trypanosoma brucei*. *Mol. Biochem. Parasitol.* **99**, 89-101.

Woodward, R. and Gull, K. (1990). Timing of nuclear and kinetoplast DNA replication and early morphological events in the cell cycle of *Trypanosoma brucei*. *J. Cell Sci.* **95**, 49-57.

Zeng, C., Kouprina, N., Zhu, B., Cairo, A., Hoek, M., Cross, G. A. M., Osoegawa, K., Larionov, V. and de Jong, P. (2001). Large-insert BAC/YAC libraries for selective re-isolation of genomic regions by homologous recombination in yeast. *Genomics* **77**, 27-34.